DMD Fast Forward. Published on September 19, 2006 as doi:10.1124/dmd.106.010827

Investigation of structure and function of a catalytically efficient variant of the human flavin-containing monooxygenase form 3 (FMO3)

TÍMEA BORBÁS, JUN ZHANG, MATT A. CERNY, ISTVÁN LIKÓ AND JOHN R. CASHMAN

Human BioMolecular Research Institute, San Diego, California (J.Z., M.C., J.R.C.); and Division of Pharmacology and Drug Safety, Gedeon Richter Ltd., Budapest, Hungary (T.B., I.L.)

Running title: Structure-function studies of L360P FMO3.

Corresponding author:

John R. Cashman

Human BioMolecular Research Institute

5310 Eastgate Mall, San Diego, CA 92121

Email: JCashman@hbri.org

Number of text pages: 26

Number of Tables: 4

Number of Figures: 3

Number of References: 46

Number of words in Abstract: 265

Number of words in Introduction: 613

Number of words in Discussion: 1615

Abbreviations used are:

FMO, flavin-containing monooxygenase; maltose-binding fusion proteins (i.e., MBP) C-terminal poly-histidine (His_6) fusion protein (MBP-FMO3-His_6); SNPs, single nucleotide polymorphisms, SDS-PAGE, sodium dodecyl sulfate polyacrylamide gel electrophoresis; TMA, trimethylamine; TMA *N*-oxide, trimethylamine N-oxide; MMI, mercaptoimidazole; 5-DPT, 10-[(N,N-dimethylaminopentyl)-2-(trifluoromethyl)]phenothiazene, DETAPAC, diethylenetriaminepentaacetic acid; PDB, Protein Data Bank; 1get, glutathione reductase; 1npx, NADPH-peroxidase; 1vqw, a protein with similarity to flavin-containing monooxygenases; 1w4x, phenylacetone monooxygenase.

DMD Fast Forward. Published on September 19, 2006 as DOI: 10.1124/dmd.106.010827
This article has not been copyedited and formatted. The final version may differ from this version.

Abstract

To characterize the contribution of amino acid 360 to the functional activity of the human flavin-containing monooxygenase form 3 (FMO3) and form 1 (FMO1) in the oxygenation of drugs and chemicals, we expressed four FMO3 variants (i.e., Ala^{360}-FMO3, His^{360}-FMO3, Gln^{360}-FMO3 and Pro^{360}-FMO3) and one FMO1 variant (i.e., Pro^{360}-FMO1) and compared them to wild-type enzymes (Leu^{360}-FMO3 and His^{360}-FMO1), respectively. The amino acid substitutions were introduced into wild-type FMO3 or FMO1 cDNA by site directed mutagenesis. The thermal stability of variants of Leu^{360} FMO3 was also studied and the thermal stability was significantly different from that of wild-type FMO3. The influence of different substrates to modulate the catalytic activity of FMO3 variants was also examined. Selective functional substrate activity was determined with mercaptoimidazole, chlorpromazine and 10-[(N,N-dimethylaminopentyl)-2-(trifluoromethyl)] phenothiazene. Compared with wild-type FMO3, the Ala^{360}-FMO3, and His^{360}-FMO3 variants were less catalytically efficient for mercaptoimidazole *S*-oxygenation. *N*-Oxygenation of chlorpromazine was significantly less catalytically efficient for His^{360}-FMO3 compared with wild-type FMO3. Human Pro^{360}-FMO1 was significantly more catalytically efficient at *S*-oxygenating mercaptoimidazole and chlorpromazine compared with wild-type FMO1. The data support the mechanism that the Pro^{360} loci affect thermal stability of FMO3. Because different amino acids at position 360 affect substrate oxygenation in a unique fashion from that of FMO3 stimulation, we conclude that the mechanism of stimulation of FMO3 is distinct from that of enzyme catalysis. A molecular model of human FMO3 was also constructed to help explain the results. The increase in catalytic efficiency observed for

Pro^{360} in human FMO3 was also observed when the His of FMO1 was replaced by Pro at loci 360.

Introduction

The flavin-containing monooxygenases (FMOs; 1.14.13.8) are a family of drug metabolizing enzymes which utilize FAD, NADPH and molecular oxygen to catalyze the oxygenation of a large number of drugs, pesticides and other xenobiotics containing soft nucleophiles (Cashman and Zhang, 2002; Krueger and Williams, 2005). Generally, FMOs are detoxication catalysts that convert relatively non-polar compounds to more polar metabolites via the incorporation of one atom of molecular oxygen (Ziegler, 1988). Eleven human *FMO* genes have been identified, although only five forms of the enzyme have been shown to be functionally active (Hernandez *et al.*, 2004; Hines *et al.*, 2002). Of the five functionally active FMOs, FMO3 (Lomri *et al.*, 1992) and FMO5 (Zhang and Cashman, 2006) appear to be the prominent members in the adult human liver. It is likely that the role in FMO-mediated metabolism by either FMO3 or FMO5 is dependent on the type of substrate presented to the enzyme (Cashman and Zhang, 2006).

For FMO3, certain single nucleotide polymorphisms (SNPs) are associated with significant functional differences in enzyme activity (Cashman and Zhang, 2006). Certain amines, including drugs, dietary agents and xenobiotics metabolized by FMO3 as a prominent metabolic pathway may be significantly altered if an FMO3 SNP is present (Kang *et al.*, 2000; Cashman *et al.*, 2001; Cashman, 2002; Park *et al.*, 2002). For example, humans normally *N*-oxygenate approximately >96.5 % of benzydamine in an FMO3-dependent process. For individuals with defective FMO3, a 2.7-3.3-fold decrease in the average percentage of benzydamine N-oxide formation has been observed (Mayatepek *et al.*, 2004). The metabolism of trimethylamine (TMA) illustrates another example of a dramatic effect on FMO3-mediated metabolism where individuals that

possess defective FMO3 decrease TMA *N*-oxygenation. Because FMO3 is solely responsible for TMA *N*-oxygenation in vivo, mutations of FMO3 that cause defective TMA *N*-oxygenation lead to a rare metabolic disorder called trimethylaminuria (Dolphin *et al*., 1997; Cashman, 2002a; Cashman *et al*., 2003). In addition to rare mutations that cause trimethylaminuria, common SNPs can also decrease FMO3-mediated metabolism and have clinical consequence (Koukouritaki, *et al*., 2005). In the case of sulindac and chemoprevention of colorectal cancer, for example, FMO3 SNPs may improve the overall clinical efficacy of the drug. The active sulfide metabolite of sulindac (i.e., sulindac sulfide) is *S*-oxygenated to the S-oxide and then to the sulfone by FMO3 (Hamman *et al*., 2000). SNPs of FMO3 at the E158K and E308G loci decrease functional activity of FMO3 and decrease the retro-oxygenation of sulindac sulfide to inactive sulfoxide and increase the efficacy of sulindac. Among sulindac-treated patients that did not develop familial adenomatous polyposis, 33 % were homogenous for E158K and 17 % were homozygous for E308G variants (Hisamuddin *et al*., 2004).

Common FMO3 SNPs vary widely across ethnic groups and it is possible that interethnic variation contributes to therapeutic drug variability for drugs metabolized by FMO3 (Cashman *et al*., 2001; Furnes *et al*., 2003). For example, certain ethnic groups have a much greater prevalence of common FMO3 SNPs and possess a greater incidence of abnormal TMA *N*-oxygenation (Mitchell *et al*., 1997). A rare Leu360Pro FMO3 SNP has only been observed in individuals of African descent (Lattard *et al*., 2003). cDNA-expression of the enzyme showed that Pro^{360}-FMO3 possessed an extensive metabolizer phenotype in vitro. Thus, mutation of Leu^{360} of FMO3 to a Pro is an example of a

mutation that has been shown to have a higher V_{max} for several substrates with little effect on the K_m (Lattard *et al.*, 2003). Our recent discovery of this pharmacologically important polymorphism led us to explore further the affect of other amino acid substitutions at position 360 of FMO3 and create a molecular model to help understand the physical properties and the affinity, stimulation and turnover of a number of known FMO3 substrates.

DMD Fast Forward. Published on September 19, 2006 as DOI: 10.1124/dmd.106.010827
This article has not been copyedited and formatted. The final version may differ from this version.

Materials and Methods

Chemicals. Mercaptoimidazole (MMI), chlorpromazine HCl and all other chemicals and reagents were purchased from Aldrich Chemical Co. (Milwaukee, WI) in the highest purity commercially available. The components of the NADPH generating system were obtained from Sigma Chemical Co. (Milwaukee, WI). Buffers and other agents were purchased from VWR Scientific, Inc., (San Diego, CA). The phenothiazene analog 10-[(N,N-dimethylaminopentyl)-2-(trifluoromethyl)]phenothiazene (5-DPT) was synthesized by the method previously described (Brunelle *et al.,* 1997).

Cloning and Expression. Wild-type human FMO3 and several variants including Ala^{360}-FMO3, His^{360}-FMO3, Gln^{360}-FMO3, Pro^{360}-FMO3 and wild-type human FMO1 and its variant Pro^{360}-FMO1 were expressed as fusion proteins containing N-terminal maltose-binding protein and C-terminal poly-histidine tags (MBP-FMO3-His_6 and MBP-FMO1-His_6, respectively) as described previously (Lattard *et al*., 2004; Brunelle *et al*., 1997). *E. coli* JM109 cells were transformed with the pMAL-FMO-His_6 plasmid and grown at 37 °C in SOC medium (2 % bacto tryptone, 0.5 % yeast extract, 8 mM NaCl, 10 mM $MgCl_2$, 2.5 mM KCl, 20 mM glucose) to an absorbance of 0.5-0.6 at 600 nm. 0.2 mM isopropyl β-thio galactopyranoside, 0.05 mM riboflavin and 100 μg/ml ampicillin were then added. The cells were further incubated overnight at 30 °C. Cells were harvested by centrifugation at 6000 g for 10 min and resuspended in lysis buffer (50 mM Na_2HPO_4, pH 8.4; 0.5 % Triton X-100) containing 0.2 % L-α-phosphatidylcholine, 0.5 mM phenylmethylsulfonylfluoride and 100 mM flavin adenine dinucleotide. After incubation for 30 min at 4 °C, the resuspended cells were disrupted by

sonication (i.e., three 2-min bursts separated by periods of cooling). The solution was centrifuged at 18,000 g for 30 min at 4 °C. The resulting supernatant was placed onto an amylose column (New England Bio Lab, Beverly, MA). The pellets were extracted one more time as described above. The resulting supernatant was loaded onto the same amylose column and eluted as described below.

Purification of MBP-FMO-His$_6$ Fusion Proteins. All purification procedures were carried out at 4 °C. The resulting supernatants were applied (0.5 ml/min) to an amylose column (35 ml) equilibrated with Buffer A (50 mM Na_2HPO_4 pH 8.4; 0.5 % Triton X-100). The column was washed with five volumes of Buffer A containing 100 mM flavin adenine dinucleotide. Bound proteins were eluted with 10 mM maltose in Buffer A containing 100 mM flavin adenine dinucleotide. Eluted fractions were then applied to a HisTrap Chelating column (HisTrap Kit; Amersham Biosciences, Piscataway, NJ) equilibrated with buffer B (20 mM phosphate, pH 7.4, 0.5 M NaCl, 10 mM imidazole and 0.5 % Triton X-100) according to the manufacturer's specifications. After washing with buffer B, bound proteins were eluted with 200 mM imidazole in buffer B. Eluted protein was fractionated by SDS-PAGE (Laemmli, 1970) and visualized with Coomasie Blue staining. The fractions containing the *bis*-fusion protein were pooled and precipitated by adding PEG 500 to achieve a final concentration of 20 % PEG (w:v) and incubated on ice for 30 min. The PEG-precipitated protein was collected by centrifuging at 18,000 rpm for 20 min. The protein was resuspended in buffer A containing 100 mM flavin adenine dinucleotide and 10 % glycerol at 4 °C. The

DMD Fast Forward. Published on September 19, 2006 as DOI: 10.1124/dmd.106.010827
This article has not been copyedited and formatted. The final version may differ from this version.

total protein concentration was measured by bicinchoninic acid assay (Pierce Inc., Rockford, IL) using serum bovine albumin as a standard.

Determination of MBP-FMO-His$_6$ concentration by SDS-PAGE and Commassie Blue Staining. SDS-PAGE was done as described by Laemmli (1970). MBP-FMO1-His$_6$ and MBP-FMO3-His$_6$ were quantified by Commassie Blue staining and compared with a Bovine Serum Albumin (BSA) standard. Briefly, MBP-FMO-His$_6$ proteins and different quantities of standard BSA (i.e., 2, 1.5, 1.0, 0.5, and 0.1 µg per lane) were fractionated by electrophoresis on a 10 % polyacrylamide gel under denaturing conditions and stained with Commasie Blue. After destaining, FMO quantification was done by densitometry analysis employing Scion Image software (public domain, http://www.scioncorp.com/). The relationship between the relative intensity of the detected signal and the amount of FMO was linear (r^2=0.9).

Enzyme Assays. The oxygenation of MMI was determined by monitoring the oxidation of NADPH associated with *S*-oxygenation of this substrate (Dixit and Roche, 1984). The assay contained 50 mM sodium phosphate buffer (pH 8.4), 0.5 mM diethylenetriaminepentaacetic acid (DETAPAC), 0.2 mM NADPH and 0-0.1 mg MBP-FMO-His$_6$. Reactions were initiated by the addition of substrate and monitored at 340 nm after obtaining a stable baseline. Kinetic parameters for MMI *S*-oxygenation were obtained from individual experiments after the addition of decreasing amounts of substrate (1000, 250, 50, 25, 12.5, 6.25, 3.125 μM final concentration) to the sample cuvette.

DMD Fast Forward. Published on September 19, 2006 as DOI: 10.1124/dmd.106.010827
This article has not been copyedited and formatted. The final version may differ from this version.

The *N*-oxygenation of chlorpromazine or 5-DPT was also determined as previously described (Lomri *et al.,* 1993; Brunelle *et al.,* 1997). Briefly, a typical incubation mixture contained 50 mM potassium phosphate buffer (pH 8.4), 0.4 mM $NADP^+$, 0.4 mM glucose-6-phosphate, 1 IU glucose-6-phosphate dehydrogenase, 0.8 mM DETAPAC and 0-0.9 mg MBP-FMO-His_6. Reactions were initiated by the addition of 5-DPT or chlorpromazine, incubated at 37 °C for 20 min and stopped by addition of 4 volumes of cold dichloromethane. After addition of 20 mg of Na_2CO_3 the incubations were mixed and centrifuged to partition metabolites and remaining 5-DPT or chlorpromazine into the organic fraction. The organic fraction was evaporated, dissolved in methanol, mixed thoroughly, centrifuged, and analyzed by HPLC as described previously (Brunelle *et al.*, 1997). *N*-Oxygenation of 5-DPT or chlorpromazine was determined by quantifying the amount of authentic product formed by HPLC. Chromatography was done on a Hitachi HPLC fitted with a AXXIOM (Richard Scientific, Novato, CA) silica phase column (4.5 μm x 25 cm) with a mobile phase of methanol/isopropanol/60 % $HClO_4$ (55:45:0.01, v:v) and UV detection. This HPLC system separated chlorpromazine, 5-DPT, chlorpromazine N-oxide and 5-DPT N-oxide that gave retention volumes of 3.1, 2.9, 4.1, and 4.2 ml, respectively. Kinetic constants for the *N*-oxygenation of chlorpromazine were obtained from individual experiments after the addition of decreasing amounts of chlorpromazine HCl dissolved in water (600, 300, 200, 150, 127 μM final concentration).

Heat Inactivation Studies. The thermal stability of MBP-FMO3-His_6 variants and wild-type enzyme was examined by monitoring the consumption of NADPH and *S*-oxygenation of MMI. Enzyme was placed into separate test tubes containing 50 mM

phosphate buffer (pH 8.4), DETAPAC and placed on ice. The test tube was taken out of the ice and treated with heat (40 ºC) for the indicated time and then immediately returned to ice. Shortly thereafter, the heat-treated enzyme was combined with NADPH and transferred to a cuvette for a photometric assay using MMI (100 µM). Non-heat treated enzyme was used as a control to determine 100 % activity. Percent remaining activity as a function of time was determined by dividing the observed activity for the heat-treated enzyme by that of the non-heat treated enzyme.

Molecular Modeling of Human FMO3. The SWISS-MODEL system was used for carrying out homology modeling (SWISS PBD viewer, Template Selection ExPDB database and PromodII) (Schwede *et al*., 2003; Guex and Peitsch, 1997; Peitsch, 1995). Four PDB (Protein Data Bank) (Berman *et al*., 2000) structures were selected for homology modeling the structure of human FMO3: glutathione reductase (1get) (Mittl *et al*., 1994), NADPH-peroxidase (1npx) (Stehle *et al*., 1991), a protein with similarity to flavin-containing monooxygenases (1vqw) (Eswaramoorthy *et al*., 2006) and phenylacetone monooxygenase (1w4x) (Malito *et al*., 2004). Several FMO sequences were involved in the analysis (i.e., including FMO3 of human, rat, cow, bull, chicken and mouse, FMO1 of human, rat and mouse, and rabbit FMO2). Secondary structure was predicted with different methods.

Data analysis. The estimation of kinetic parameters was achieved by the incubation of at least 5 different substrate concentrations with MBP-FMO-His_6. Incubations were done in duplicate or triplicate. Data were analyzed with nonlinear regression curve fit tools in Graphpad software using Michaelis-Menten model. The ordinary least-squares criterion was used to fit the Michaelis-Menten model to the data,

taking velocity as the dependent variable. The minimum values of the sum of squared residuals were computed using NAG foundation library routine EO4FDF (Numerical Algorithms group Ltd., Natick, MA), a combined Gauss-Newton and modified Newton algorithm, using function values only. Data are presented as the mean ± standard deviation from separate experiments. Statistical analysis was done using GraphPad 2.01 (GraphPad Software, Inc., San Diego, CA). Kruskal-Wallis statistical analysis was run in order to compare values for FMO3 variants versus values for wild-type FMO3 enzyme. Mann Whitney test was run in order to compare values for FMO1 variant with wild-type enzyme versus wild-type FMO1 enzyme. Two way ANOVA with Bonferroni post-hoc test were run in order to determine the effect of isoform and modulators on enzyme activity and the interaction of these factors. The confidence interval selected was chosen to be 95 %.

DMD Fast Forward. Published on September 19, 2006 as DOI: 10.1124/dmd.106.010827
This article has not been copyedited and formatted. The final version may differ from this version.

Results

Previously, the human FMO3 gene variant *Pro^{360}-FMO3* was observed only in individuals of African descent, as identified by either MassEXTEND (i.e., a high-throughput chip-based genotype variation detection method) with matrix-assisted laser desorption ionization time-of-flight mass spectrometry described before (Cashman *et al*., 2001) or by DNA re-sequencing (Lattard *et al*., 2003). For the African American population examined, the Pro^{360}-FMO3 allele frequency was 0.019. cDNA-expresssion of the Pro^{360}-FMO3 showed the variant was about 2 to 4-fold more catalytically efficient in the oxygenation of prototypical substrates compared with wild-type enzyme (Lattard *et al*., 2003). For human FMO3, the leucine at loci 360 is not conserved among different species and different FMO isoforms. In mouse and rabbit FMO3, the 360 position is substituted with glutamine. In FMO1, the position is replaced with histidine and is conserved among different species (i.e., human, mouse, rabbit and pig). To investigate whether the 360 position plays a regulatory role for FMO function, site-directed mutagenesis was used to construct and express four human FMO3 variants and one variant of human FMO1 for comparison with wild-type FMO3 and FMO1, respectively. The four variants were selected based on the idea of a simple alanine replacement, a histidine replacement to mimic FMO1, a glutamine replacement to mimic FMO3 in rodents, and a proline to represent the L360P FMO3 SNP identified in an African American population.

Several FMO3 variants (i.e., Ala^{360}, His^{360}, Gln^{360} and Pro^{360}) and a single FMO1 variant (i.e., Pro^{360}) were introduced into wild-type FMO3 and FMO1 cDNA, respectively. These mutants, along with wild-type FMOs were over-expressed as MBP-

DMD Fast Forward. Published on September 19, 2006 as DOI: 10.1124/dmd.106.010827
This article has not been copyedited and formatted. The final version may differ from this version.

FMO-His_6 fusion proteins in *E. coli* JM-109 and purified as described in the *Materials and Methods*. Enzyme fractions were purified to approximately 90 % purity and used for kinetic studies.

Preliminary studies showed that human MBP-FMO3 supplemented with NADPH catalyzed the rapid oxygenation of MMI, chlorpromazine and 5-DPT to their corresponding S-oxide or tertiary amine N-oxides, respectively. The formation of product was a linear function of protein concentration (0-0.16 mg of wild-type FMO3 protein, 0-0.35 mg of Ala^{360}-FMO3, 0-0.9 mg of His^{360}-FMO3, 0-0.5 mg of Gln^{360}-FMO3 and 0-0.15 mg of Pro^{360}-FMO3) and with incubation time for at least 10 min. Similarly, formation of oxygenation products by human FMO1 was a linear function of protein concentration (0-0.05 mg of wild-type FMO1 and 0-0.03 mg of Pro^{360}-FMO1) and with incubation time for at least 8 min.

The thermal stability of variants of FMO3 at loci 360 was investigated. Ala^{360}-FMO3, His^{360}-FMO3 and Pro^{360}-FMO3 were compared with wild-type FMO3 by examining MMI *S*-oxygenation (Figure 1). FMO3 enzymes were treated at 40 ºC in the absence of NADPH at various times (0-60 sec) and the percent remaining MMI *S*-oxygenation activity was determined by monitoring NADPH consumption spectrophotometrically. Data were analyzed with nonlinear regression curve fit tools in Graphpad software using one phase exponential decay. The half lives were determined and compared by F-test. The half life was 37.28, 69.55, 26.62 and 11.54 min, for wild-type FMO3, Pro^{360}-FMO3, His^{360}-FMO3 and Ala^{360}-FMO3, respectively. The F-test showed significant differences between the groups ($p<0.0001$). Compared with wild-type

DMD Fast Forward. Published on September 19, 2006 as DOI: 10.1124/dmd.106.010827
This article has not been copyedited and formatted. The final version may differ from this version.

enzyme, Ala^{360}-FMO3 appeared to be the most sensitive variant to thermal inactivation (Figure 1).

Detailed kinetic studies were done with the FMO3 variants and compared with wild-type enzyme. The K_m and V_{max} values obtained for each variant are summarized in Tables 1 and 2. As shown by the kinetic constants listed in Table 1, MMI was an excellent substrate for the wild-type FMO3 having an apparent K_m of 18.1 μM and V_{max} of 30.3 nmol/min/mg of enzyme. To examine the effect of position 360 amino acid variants, the *S*-oxygenation of MMI was determined by measuring NADPH consumption.

Compared with wild-type FMO3, the catalytic efficiency (i.e., V_{max}/K_m) of Ala^{360}-FMO3, His^{360}-FMO3 and Gln^{360}-FMO3 was approximately a third or less of the value. The catalytic efficiency of Pro^{360}-FMO3 was greater than wild-type FMO3. Kruskal-Wallis statistical analysis showed that the Ala^{360}-FMO3, His^{360}-FMO3 variants were significantly different compared with wild-type FMO3.

To examine the influence of the Pro^{360} substitution on a closely related enzyme, wild-type human FMO1 was converted into Pro^{360}-FMO1 by site-directed mutagenesis. As shown in Table 1, the catalytic efficiency of Pro^{360}-FMO1 was greater than three-fold that of wild-type FMO1. The Mann Whitney test showed the Pro^{360}-FMO1 variant was significantly different than wild-type enzyme.

Chlorpromazine was used to investigate the ability of each variant to catalyze the *N*-oxygenation of a tertiary amine to its N-oxide. Chlorpromazine N-oxide formation was monitored by analysis of organic extracts of incubation mixtures by HPLC. Compared with wild-type FMO3, Ala^{360}-FMO3 and Gln^{360}-FMO3 *N*-oxygenated chlorpromazine with similar catalytic efficiency (Table 2). His^{360}-FMO3 *N*-oxygenated

DMD Fast Forward. Published on September 19, 2006 as DOI: 10.1124/dmd.106.010827
This article has not been copyedited and formatted. The final version may differ from this version.

chlorpromazine with less catalytic efficiency than wild-type enzyme and this was confirmed by Kruskal-Wallis statistical analysis. Pro^{360}-FMO3 was twice as catalytically efficient compared with wild-type enzyme. The decrease in V_{max}/K_m for His^{360}-FMO3 was largely due to a lower V_{max} value suggesting a decrease in turnover for the tertiary amine. The increase in catalytic efficiency for Pro^{360}-FMO3 compared with wild-type enzyme was largely due to a decrease in K_m suggesting an increase in the affinity of the enzyme for the tertiary amine.

In agreement with that observed for FMO3, chlorpromazine *N*-oxygenation was more efficient for Pro^{360}-FMO1. As shown in Table 2, the catalytic efficiency of Pro^{360}-FMO1 was 38 % greater than wild-type FMO1. As judged by the Mann Whitney test the values for Pro^{360}-FMO1 were significantly different than wild-type enzyme. The difference in catalytic efficiency apparently was due to changes in both K_m and V_{max}.

Previously, it was reported that imipramine and chlorpromazine stimulated the FMO3-dependent *S*-oxygenation of MMI (Wyatt *et al.,* 1998). If the Pro^{360} amino acid is proximal to the positive regulatory site then alteration of this amino acid could influence FMO-dependent stimulation of substrate oxygenation. Table 3 showed that wild-type FMO3-catalyzed MMI *S*-oxygenation was stimulated by chlorpromazine. However, of the Leu^{360}-FMO3 variants examined, compared to non-stimulated enzyme, none showed a statistically significant stimulation of MMI *S*-oxygenation on the basis of two-way ANOVA and a Bonferroni post-hoc test. In all cases examined, the degree of stimulation was less than that observed for wild-type FMO3.

Data of Table 4 shows the effect of chlorpromazine on the *N*-oxygenation of the tertiary amine 5-DPT as well as the effect of 5-DPT on the *N*-oxygenation of

chlorpromazine. Chlorpromazine stimulated the FMO3-mediated *N*-oxygenation of 5-DPT but the effect was dependent on the amino acid substitution at position 360 and this effect did not reach statistical significance. The rank order of stimulation of FMO3-mediated 5-DPT *N*-oxygenation was: His^{360}-FMO3 > Gln^{360}-FMO3 > Ala^{360}-FMO3 >> Pro^{360}-FMO3 = wild-type FMO3. In contrast, in the presence of 5-DPT, chlorpromazine *N*-oxygenation was decreased and this was judged to be statistically significant on the basis of two-way ANOVA and a Bonferroni post-hoc test. The rank order stimulation was as follows: Pro^{360}-FMO3 = Gln^{360}-FMO3 = Ala^{360}-FMO3 = wild-type FMO3 > His^{360}-FMO3.

Molecular modeling of the human FMO3 structure was done in an attempt to understand the possible interaction of the amino acid at position 360 with the NADPH or FAD cofactors. Four PDB structures were selected for homology modeling the structure of human FMO3. Glutathione reductase (1get) and NADPH-peroxidase (1npx) were used because they were used in a previous study (Cashman, 2002b). Two other structures were suggested by the SWISS-MODEL Template Selection ExPDB database (Schwede *et al*., 2003; Guex and Peitsch, 1997; Peitsch, 1995) (i.e., a protein with similarity to flavin-containing monooxygenases (1vqw) and phenylacetone monooxygenase (1w4x)). The four PDB structures were manually aligned and superimposed. Two conserved domains of the FAD binding domain and the NADPH binding domain could be found in the superimposed structures (Figure 2). With the exception of these domains, the structures were quite divergent.

The alignment of FMOs was based on sequence homology and secondary structure of several FMO sequences (i.e., including FMO3 of human, rat, cow, bull,

chicken and mouse, FMO1 of human, rat and mouse, and rabbit FMO2). Next, the alignment was done combining the four known substructures with the alignment of the FMOs. The secondary structure elements (α-helix and β-sheets) showed good alignment and considerable sequence similarity in the common structural elements (i.e., FAD and NADPH binding domains). This alignment was used as a starting point for building the human FMO3 model structure and these data were sent to the Swiss-model server and the PromodII program to calculate the 3D model structure of human FMO3 (Schwede *et al*., 2003; Guex and Peitsch, 1997; Peitsch, 1995).

The molecular model derived is shown in Figure 3. Based on the model, Leu^{360} lies near but it is not in direct contact with the FAD adenine moiety. The amino acids of the reference structures corresponding to Leu^{360} of human FMO3 (i.e., 1get T293, 1vqw Y325, 1W4X T425, 1NPX T271) also showed that the corresponding amino acid was proximal to the FAD (data not shown).

Discussion

Human FMO3 oxygenates a variety of nucleophilic primary, secondary and tertiary amines as well as sulfur and other heteroatom-containing chemicals and drugs (Krueger and Williams, 2005). Because human FMO3 is not readily induced or inhibited, variation in the functional activity comes from genetic variability arising largely from common SNPs (Cashman, 2002a). On the other hand, individuals with rare *FMO3* mutations that cause defective TMA *N*-oxygenation suffer from trimethylaminuria. It is the *FMO3* allelic variation present in common genetic polymorphisms that have been reported to affect chemical and drug metabolism mediated by FMO (Cashman and Zhang, 2006; Koukouritaki and Hines, 2005; Treacy *et al.*, 1998; Akerman *et al*., 1999; Dolphin *et al*., 2000). In addition, a detailed examination of structure and function of common allelic variation could also provide insight into mechanistic or structural aspects of FMO action.

In a previous study, a few individuals (i.e., 1 %) were identified as possessing the Pro^{360}-FMO3 variant and we reported Pro^{360}-FMO3 was more catalytically efficient than wild-type FMO3 (Lattard *et al*, 2003). Pro^{360}-FMO3 oxygenated MMI, TMA and 5-DPT approximately 3-, 5- and 2-fold more efficiently, respectively, than wild-type FMO3. For these substrates, the K_m values for Pro^{360}-FMO3 and wild-type enzyme were similar but the V_{max} values were greater. It is possible that Pro^{360}-FMO3 could facilitate desorption of $NADP^+$ or dehydration of FAD pseudobase water and thus speed up the FMO reaction. Evidence that one or the other of these processes is the rate-limiting step in FMO catalysis has been reported previously (Poulsen and Ziegler, 1979; Beaty and Ballou,

1981). Another possibility is that Pro^{360}-FMO3 has an affect on the structure of FMO3 because it is known that substitution of a Pro into an enzyme can change protein structure. We did observe a significant difference in the effect of 360 amino acid substitution on the thermal stability and half life of Leu^{360}-FMO3 variants (Figure 1) and we suspect the effect of the 360 loci substitution has a key effect on function. Accordingly, detailed kinetic studies were undertaken.

We examined variants at the 360 loci to gain insight into structural features that may contribute to increasing the catalytic efficiency of Pro^{360}-FMO3. Compared with wild-type human FMO3, Pro^{360}-FMO3 *S*-oxygenated MMI with greater catalytic efficiency. Ala^{360}-FMO3, His^{360}-FMO3, and Gln^{360}-FMO3 variants all showed less catalytic efficiency compared with wild-type enzyme (Table 1). *N*-Oxygenation of chlorpromazine with the Pro^{360} variant was more catalytically efficient than the wild-type enzyme. His^{360}-FMO3 but not Ala^{360}-FMO3, and Gln^{360}-FMO3 were less catalytically efficient than wild-type enzyme at chlorpromazine *N*-oxygenation (Table 2).

We also examined variants of human FMO1 at the 360 loci to see if the observations about FMO3 extended to human FMO1. The Pro^{360}-FMO1 variant catalyzed the *S*-oxygenation of MMI with greater catalytic efficiency than wild-type enzyme (Table 1). Likewise, Pro^{360}-FMO1 was more catalytically efficient at *N*-oxygenating chlorpromazine than wild-type enzyme (Table 2). Thus, in a similar vein as human FMO3, replacement of the His^{360} of human FMO1 with Pro^{360} affords an enzyme with greater catalytic efficiency. Because human FMO1 and FMO3 share 53 % sequence identity (Lawton *et al*., 1994), it is not surprising that the factors at loci 360 that work to increase catalytic efficiency in FMO3 are also at work for FMO1.

It has been reported that tertiary amines such as chlorpromazine and imipramine stimulate oxygenation of other FMO3 substrates such as MMI (Wyatt *et al.*, 1998). The data pointed to a regulatory site for FMO3 that facilitated substrate turnover (Cashman, 1995). In the study herein, we observed significant stimulation by chlorpromazine of MMI *S*-oxygenation in the presence of wild-type FMO3 but Ala^{360}-FMO3, His^{360}-FMO3, Gln^{360}-FMO3, and Pro^{360}-FMO3 variants did not show a statistically significant effect (Table 3). In the presence of chlorpromazine, wild-type FMO3 mediated MMI *S*-oxygenation was stimulated 24 %. By a simple substitution of Leu^{360} in wild-type FMO3 for Ala^{360}-, His^{360}-, Gln^{360}- or Pro^{360}-FMO3, the enzyme lost its responsiveness to stimulation. In summary, for MMI *S*-oxygenation, the 360 loci of FMO3 can contribute to modulation of stimulation in the presence of chlorpromazine but the effect is not a simple matter of hydrophobic or basic interactions. The mechanism responsible for an increase in catalytic efficacy by substitution of Pro at loci 360 appears to be distinct from that of enzyme stimulation.

We also examined the influence of chlorpromazine to stimulate 5-DPT *N*-oxygenation as well as the influence of 5-DPT to stimulate chlorpromazine *N*-oxygenation. In the case of variants Ala^{360}-FMO3, His^{360}-FMO3 and Gln^{360}-FMO3 the *N*-oxygenation of 5-DPT was stimulated in the presence of chlorpromazine but this did not reach statistical significance (Table 4). The fact that both aliphatic and basic amino acid substitution at loci 360 cause a similar percent stimulation of FMO3 suggests that the mechanism of enzyme stimulation of FMO3 may involves multiple structural effects. The effect of amino acid substitution on stimulation of substrate oxygenation as a

DMD Fast Forward. Published on September 19, 2006 as DOI: 10.1124/dmd.106.010827
This article has not been copyedited and formatted. The final version may differ from this version.

consequence of changes at loci 360 is quite distinct for MMI and 5-DPT and suggests that these substrates are handled differently by FMO3.

In the presence of 5-DPT, the 360 loci variants and wild-type FMO3 enzymes decreased chlorpromazine *N*-oxygenation (Table 4). We interpret this as alternate substrate competitive inhibition of 5-DPT on chlorpromazine *N*-oxygenation. Previously, we showed that compared to 5-DPT, chlorpromazine was an inferior substrate for FMO3 likely due to the shorter aliphatic side chain associated with this tertiary amine (Lomri *et al*., 1993). In contrast, 5-DPT possesses a more optimal aliphatic side chain length to place the tertiary amine further into the substrate binding channel of FMO3 and afford more efficient *N*-oxygenation. That no stimulation of *N*-oxygenation of chlorpromazine by 5-DPT was observed and in fact, alternate competitive substrate inhibition was observed, suggests that the mechanism of alternate substrate stimulation is distinct from that of alternative tertiary amine *N*-oxygenation (or alternative substrate competitive inhibition).

Two FMO models were previously reported (Cashman, 2002b, Ziegler, 2002) using glutathione reductase (Mittl *et al*., 1994) and NADPH peroxidase (Stehle *et al*., 1991) structures as templates. The previously developed human FMO3 models were based on threading the FMO3 sequence onto the X-ray structure of the flavoproteins whereas the model developed herein was based on homology modeling using the cofactor binding domains as key linchpins. The recently published structures of phenylacetone monooxygenase (i.e., a Baeyer-Villiger monooxygenase) (Malito *et al*., 2004) and structures of the FMO from *Schizosaccharomyces pombe* (Eswaramoorthy *et al*., 2006) encouraged us to construct a new human FMO3 model. Comparison of the FMO3

sequences with other monooxygenases of known structures revealed well-defined FAD- and $NADP^+$ binding domains that were readily modeled. In our model as well as the earlier models these cofactor domains have typical dinucleotide-binding folds and other known conserved structural motifs as part of these domains (Krueger and Williams, 2005). Based on the prior model, we proposed that FMO3 amino acid 360 is near the FAD cofactor region (Figure 3). Leucine 360 is proximal but not in direct contact with the FAD. This amino acid may be involved in domain rotation thought to be occurring during catalysis (Malito *et al*, 2004; Ballou *et al*., 2006). We interpret the amino acid substitution at position 360 as having an influence on dehydration of the FAD pseudo base. If amino acid 360 has a determining role in the flexibility of FMO3 then this amino acid may have an influence on $NADP^+$ desorption

Beyond the conserved domains there are insertions that are unique in mammalian FMOs compared to other monooxygenases. A 40 residue polypeptide chain segment insertion in the FAD binding domain occurs in the interface between the two domains. The C-terminus of the FAD binding domain contains mostly α-helical polypeptide chains that extend from the FAD domain to the NADPH domain. In addition, the NADPH binding domain exhibits an insertion of 66 amino acids right after the βαβ NADPH binding unit. The position of this insertion is the same as in the Baeyer-Villiger monooxygenase (Malito *et al.*, 2004), but the insertion is shorter in the FMO and contains only two α-helixes. These insertions might play a role in substrate binding and the catalytic mechanism of human FMO's but delineating this will require further refinement of the model structures.

In summary, for human FMO3, inter-individual variation of enzymatic activity can contribute to discernible differences in drug or chemical metabolism (Cashman and Zhang, 2002). Genetic polymorphisms of genes encoding FMO enzymes resulting in "fast metabolizer" phenotype may lead to rapid drug metabolism and potentially a decrease in therapeutic efficacy of drugs. Based on the kinetics and the molecular model, the change in catalytic efficacy as a function of modulation of amino acid position 360 is likely due to changes in the function of FAD but further refinement is required for more detailed structural analysis (i.e., substrate binding or influence of mutations on structures). In contrast to MMI that moves into the active site domain, it is possible that because the phenothiazene ring system of 5-DPT is precluded from entering the putative substrate binding domain, amino acid interactions in this region of the protein modulate the extent of substrate stimulation. The results for effects of amino acid substitution on FMO3 catalytic efficiency were distinct from those observed for stimulation of MMI *S*-oxygenation by chlorpromazine. We interpret this to suggest that the contribution of the 360 loci for FMO3 substrate stimulation is different from that of the influence of the 360 loci on FMO catalysis.

Because the 360 loci variant thus far has only been found in individuals of African descent, the functional variation of Leu^{360}-FMO3 described herein may contribute to ethnic group-dependent metabolism of chemicals and dietary materials that are FMO3 substrates. The relevance of the Pro^{360}-FMO3 SNP to human drug metabolism needs to be investigated further.

Acknowledgments.

We would like to thank Mr. Vignesh Raman for technical assistance in enzyme preparation.

References.

Akerman BR, Forrest S, Chow L, Youil R, Knight M and Treacy EP (1999) Two mutations of the *FMO3* gene in a proband with trimethylaminuria. *Hum Mutat* **13**:376-379.

Ballou DP, Entsch B, Cole LJ (2005) Dynamics involved in catalysis by single-component and two-component flavin-dependent aromatic hydroxylases. *Biochem Biophys Res Commun* **338**:590-8.

Beaty N and Ballou D (1980) A kinetic investigation of liver microsomal mixed function amine oxidase, in *Microsomes, Drug Oxidation and Chemical Carcinogenesis*, (Coon MJ, Conney AH, Estabrook RW, Gelboin HV, Gillette JR, O'Brien PJ eds) pp 209-302, Academic Press, New York, NY.

Berman HM, Westbrook J, Feng Z, Gilliland G, Bhat TN, Weissig H, Shindyalov IN, and Bourne PE (2000) The Protein Data Bank. *Nucleic Acids Research* **28**:235-242

Brunelle A, Bi YA, Lin J, Russell B, Lu YC, Berkman CE and Cashman JR (1997) Characterization of two human flavin-containing monooxygenases (form 3) enzymes expressed in *Escherichia coli* as maltose binding fusions. *Drug Metab Dispos* **25**:1001-1007.

Cashman JR, Camp K, Fakharzadeh SS, Fennessey PV, Hines RN, Mamer OA, Mitchell SC, Schlenk D, Smith RL, Tjoa SS, Williams DE and Yannicelli S (2003) Biochemical and clinical aspects of the human flavin-containing monooxygenase form 3 (FMO3) related to trimethylaminuria. *Curr Drug Metab* **4**:151-170.

Cashman JR (2002a) Human flavin-containing monooxygenase (form 3): polymorphisms and variations in chemical metabolism. *Pharmacogenomics* **3**:325-339.

Cashman JR (2002b) Flavin Monooxygenases, in *Enzyme Systems that Metabolize Drugs and Other Xenobiotics*, (Ioannides C ed) pp 67-94, John Wiley and Sons, Ltd., London.

Cashman JR and Zhang J (2002) Interindividual differences of human flavin-containing monooxygenase 3: genetic polymorphisms and functional variation. *Drug Metab Dispos* **30**:1043-1052.

Cashman JR and Zhang J (2006) Human flavin-containing monooxygenases. *Annu Rev Pharmacol Toxicol* **46**:65-100.

Cashman JR, Zhang J, Leushner J and Braun A (2001) Population distribution of human flavin-containing monooxygenase form 3: gene polymorphisms. *Drug Metab Dispos* **29**:1629-1637.

Cashman JR (1995) Structural and catalytic properties of the mammalian flavin-containing monooxygenase. *Chem Res Toxicol* **8**:165-181.

Dixit A and Roche TE (1984) Spectrophotometric assay of the flavin-containing monooxygenase and changes in its activity in female mouse liver with nutritional and diurnal conditions. *Arch Biochem Biophys* **233**:50-63.

Dolphin CT, Janmohamed A, Smith RL, Shephard EA and Phillips IR (2000) Compound heterozygosity for missense mutations in the flavin-containing monooxygenase 3 (FMO3) gene in patients with fish-odour syndrome. *Pharmacogenetics* **20**:799-807.

Dolphin CT, Janmohamed A, Smith RL, Shephard EA and Phillips IR (1997) Missense mutation in flavin-containing monooxygenase 3 gene, underlies fish-odour syndrome. *Nature Genet* **17**: 491-494.

Eswaramoorthy S, Bonanno JB, Burley SK, Swaminathan S (2006) Mechanism of action of a flavin-containing monooxygenase. *Proc Natl Acad Sci U S A* **103**:9832-9837.

Furnes B, Feng J, Sommer S and Schlenk D (2003) Identification of novel variants of the flavin-containing monooxygenase gene family in African Americans. *Drug Metab Dispos* **31**:187-193.

Guex N and Peitsch MC (1997) SWISS-MODEL and the Swiss-PdbViewer: An environment for comparative protein modeling. *Electrophoresis* **18**:2714-2723.

Hamman MA, Haehner-Daniels BD, Wrighton SA, Rettie AE, Hall SD (2000) Stereoselective sulfoxidation of sulindac sulfide by flavin-containing monooxygenases. Comparison of human liver and kidney microsomes and mammalian enzymes. *Biochem Pharmacol* **60**:7-17.

Hernandez D, Janmohamed A, Chandan P, Phillips IR, Shephard EA (2004) Organization and evolution of the flavin-containing monooxygenase genes of human and mouse; identification of novel gene pseudogene clusters. *Pharmacogenetics* **14**:117-130.

Hisamuddin IM, Whebi MA, Chao A, Wyre HW, Hylind LM, Giardiello FM and Yang VW (2004) Genetic polymorphisms of human flavin-containing monooxygenase 3 in sulindac-mediated primary chemoprevention of familial adenomatous polyposis. *Clin Cancer Res* **10**:8357-8362.

Hines RN, Hopp KA, Fanco J, Saeian K, and Begun FP (2002) Alternative processing of the human *FMO6* gene renders transcripts incapable of encoding a functional flavin-containing monooxygenase. *Mol Pharmacol* **62**:320-325.

Kang JH, Chung WG, Lee KH, Park CS, Kang JS, Shin IC, Roh HK, Dong MS, Baek HM and Cha YN (2000) Phenotypes of flavin-containing monooxygenase activity

determined by ranitidine N-oxidation are positively correlated with genotypes of linked *FM03* gene mutations in a Korean population. *Pharmacogenetics* **10**:67-78.

Koukouritaki SB, Poch MT, Cabacungan ET, McCarver DG, and Hines RN (2005) Discovery of novel flavin-containing monooxygenase 3 (FMO3) single nucleotide polymorphisms and functional analysis of upstream haplotype variants. *Mol Pharmacol* **68**:383-392.

Koukouritaki SB, Hines RN (2005) Flavin-containing monooxygenase genetic polymorphism: impact on chemical metabolism and drug development *Pharmacogenomics* **8**:807-22.

Krueger SK, Williams DE (2005) Mammalian flavin-containing monooxygenenases: structure/function, genetic polymorphisms, and role in drug metabolism. *Pharmacol Therap* **106**: 357-387.

Laemmli UK (1970) Cleavage of structural proteins during the assembly of the head of bacteriophage T4. *Nature* **227**:680-685.

Lattard V, Zhang J and Cashman JR (2004) Alternative processing events in human FMO genes. *Mol Pharmacol* **65**:1517-1525.

Lattard V, Zhang J, Tran Q, Furnes B, Schlenk D and Cashman JR (2003) Two new polymorphisms of the FMO3 gene in Caucasian and African-American populations: comparative genetic and functional studies. *Drug Metab Dispos* **31**:854-860.

Lawton M, Cashman J, Cresteil T, Dolphin C, Elfarra A, Hines RN, Hodgson E, Kimura T, Ozols J, Phillips IR, Philpot RM, Poulsen LL, Rettie AE, Shephard EA, Williams DE and Ziegler DM (1994) A nomenclature for the mammalian flavin-containing monooxygenase gene family based on amino acid sequence identity. *Arch Biochem Biophys* **308**: 254-257.

Lomri N, Gu Q, and Cashman JR (1992) Molecular cloning of flavin-containing monooxygenase (form II) cDNA from adult human liver. *Proc Natl Acad Sci USA* **89**:1685-1689.

Lomri N, Yang Z, and Cashman JR (1993) Expression in *Escherichia coli* of the flavin-containing monooxygenase D (Form II) from adult human liver: Determination of a distinct tertiary amine substrate specificity. *Chem Res Toxicol* **6**:425-429.

Malito E, Alfieri A, Fraaije MW, and Mattevi A (2004) Crystal structure of a Baeyer-Villiger monooxygenase. *Proc Natl Acad Sci USA* **101**:13157-13162.

Mayatepek E, Flock B, and Zschocke J (2004) Benzydamine metabolism in vivo is impaired in patients with deficiency of flavin-containing monooxygenase 3. *Pharmacogenetics* **14**:775-777.

Mitchell SC, Zhang AQ, Barrett T, Ayesh R, and Smith RL (1997) Studies on the discontinuous N-oxidation of trimethylamine among Jordanian, Ecuadorian and New Guinean populations. *Pharmacogenetics* **7**:45-50.

Mittl PRE, Berry A, Scrutton NS, Perham RN, and Schulz GE (1994) Anatomy of an engineered NAD-binding site. *Protein Sci* **9**:1504-14.

Park CS, Kang JH, Chung WG, Yi HG, Pie JE, Park DK, Hines RN, McCarver DG and Cha YN (2002) Ethnic differences in allelic frequency of two flavin-containing monooxygenase 3 (FMO3) polymorphisms: linkage and effects on in vivo and in vitro FMO activities. *Pharmacogenetics* **12**:77-80.

Peitsch MC (1995) Protein modeling by email. *Bio/Technology* **13**:658-660.

Poulsen LL and Ziegler DM (1979) The liver microsomal FAD-containing monooxygenase: spectral characterization and kinetic studies. *J Biol Chem* **254**:6449-6455.

Schwede T, Kopp J, Guex N and Peitsch MC (2003) SWISS-MODEL: an automated protein homology-modeling server. *Nucleic Acids Res*. **31**:3381-3385.

Stehle T, Ahmed SA, Claiborne A, and Schulz GE (1991) Structure of NADH Peroxidase from *Streptococcus Faecalis* 10C1 refined at 2.16 angstroms resolution. *J Mol Biol* **221**: 1325-1330.

Treacy EP, Akerman BR, Chow LM, Youil R, Bibeau C, Lin J, Bruce AG, Knight M, Danks DM, Cashman JR, and Forrest SM (1998) Mutations of the flavin-containing monooxygenase gene (FMO3) cause trimethylaminuria, a defect in detoxication. *Hum Mol Genet* **7**:839-845.

Wyatt MK, Overby LH, Lawton MP and Philpot RM (1998) Identification of amino acid residues associated with modulation of flavin-containing monooxygenase (FMO) activity by imipramine: structure/function studies with FMO1 from pig and rabbit. *Biochem* **37**:5930-5938.

Zhang J and Cashman, JR (2006) Quantitative analysis of FMO gene mRNA levels in human tissues. *Drug Metab Dispos* **34**:19-26.

Ziegler DM (1988) Flavin-containing monooxygenases: catalytic mechanism and substrate specificities. *Drug Metab Rev* **19**:1-32.

Ziegler DM (2002) An overview of the mechanism, substrate specificities, and structure of FMOs. *Drug Metab Rev* **34**:503-511.

Footnotes.

The financial support of the National Institute of Health (DK59618) is gratefully acknowledged. Mr. Vignesh Raman was supported by a grant from the San Diego Foundation and the James Copley Foundation.

Reprint requests should be directed to JR Cashman, Human BioMolecular Research Institute, 5310 Eastgate Mall, San Diego CA 92121.

DMD Fast Forward. Published on September 19, 2006 as DOI: 10.1124/dmd.106.010827
This article has not been copyedited and formatted. The final version may differ from this version.

Figure Legends

Figure 1. Study of the thermal stability of human FMO3 and 360 loci variants. Each enzyme was treated at 40 ºC for the indicated time. Remaining activity relative to untreated enzyme was plotted against treatment time for wild-type (■), L360P (▲), L360H (▼), and L360A (●).

Figure 2. Depiction of the conserved FAD-binding and NADPH-binding domains of the four enzymes used to create a model of human FMO3. The four enzyme structures were modeled together as indicated by different colors (i.e., 1get - green, 1vqw - yellow, 1w4x - red and 1npx - blue). The NADPH structure is colored with violet and the FAD structure is colored with magenta.

Figure 3. Molecular model of human FMO3. The color scheme (blue – turquoise – green – yellow) indicated the deviation from reference structures (i.e., blue shows the best fit), while every structural element obtained by loop search were colored in red. The coordinates of the FAD (magenta) and NADPH (violet) were imported from the 1get structure. This crude structure was acceptable for localization of amino acid 360. The atoms of Leu^{360} are represented by van der Waals spheres (i.e., the yellow colored amino acid slightly below the FAD).

TABLE 1

***S*-Oxygenation of MMI by human FMO3 and FMO1.**

The oxygenation of MMI was determined by monitoring the oxidation of NADPH associated with the *S*-oxygenation of MMI as described in *Materials and Methods*.

Data are mean ± standard deviation.

Enzyme		K_M (μM)	V_{max} (*nmol/min/mg of protein*)	V_{max}/K_m *(ml/min/mg of protein)*
FMO3 MBP	n = 6	18.1 ± 9.0	30.3 ± 6.9	1.9 ± 0.6 (100 %)[a]
Ala^{360}-FMO3 MBP	n = 9	46.1 ± 3.1*	19.7 ± 7.6	0.4 ± 0.2** (21 %)
His^{360}-FMO3 MBP	n = 9	38.2 ± 15.4	19.3 ± 7.0	0.5 ± 0.2* (26 %)
Gln^{360}-FMO3 MBP	n = 3	21.7 ± 2.2	10.4 ± 1.2	0.5 ± 0.2 (26 %)
Pro^{360}-FMO3 MBP	n = 6	33.7 ± 15.0	67.5 ± 25.3	2.7 ± 1.9 (142 %)
FMO1 MBP	n = 6	30.3 ± 7.8	12.7 ± 1.2	0.5 ± 0.1 (100 %)[b]
Pro^{360}-FMO1 MBP	n = 3	20.2 ± 1.9†	28.6 ± 3.0†	1.4± 0.3† (280 %)

[a]The values in parenthesis represent the percentage of V_{max}/K_m compared with the corresponding value for wild-type FMO3.

[b]The values in parenthesis represent the percentage of V_{max}/K_m compared with the corresponding value for wild-type FMO1.

Kruskal-Wallis statistical analysis was run in order to compare values for FMO3 variants.*$p<0.05$; ** $p<0.01$ vs. values for wild-type FMO3 enzyme.

Mann Whitney test was run in order to compare values for FMO1 variant with wild-type enzyme †$p<0.05$ vs. value for wild-type FMO1 enzyme.

DMD Fast Forward. Published on September 19, 2006 as DOI: 10.1124/dmd.106.010827
This article has not been copyedited and formatted. The final version may differ from this version.

TABLE 2

N-Oxygenation of Chlorpromazine by human FMO3 and FMO1.

The oxygenation of chlorpromazine was determined by monitoring the appearance of N-oxide associated with the *N*-oxygenation of chlorpromazine as described in *Materials and Methods.*

Data are mean ± standard deviation.

Enzyme		K_m (μM)	V_{max} (*nmol/minmg of proteinl*)	V_{max}/K_m *(ml/min/mg of protein)*
FMO3 MBP	n = 9	60.6 ± 59.5	32.0 ± 20.7	0.7 ± 0.3 (100 %)[a]
Ala^{360}-FMO3 MBP	n = 9	80.2 ± 30.5	42.6 ± 7.9	0.6 ± 0.1 (86 %)
His^{360}-FMO3 MBP	n = 12	27.6 ± 5.4	6.5 ± 5.4	0.2 ± 0.1** (29 %)
Gln^{360}-FMO3 MBP	n = 3	76.2 ± 3.6	48.5 ± 1.0	0.6 ± 0.0 (86 %)
Pro^{360}-FMO3 MBP	n = 9	26.0 ± 20.8	27.4 ± 18.3	1.2 ± 0.2 (171 %)
FMO1 MBP	n = 3	58.4 ± 3.2	175.0 ± 13.0	3.0± 0.1 (100 %)[b]
Pro^{360}-FMO1 MBP	n = 6	22.4 ± 3.0†	86.2 ± 12.6†	3.8 ± 0.5† (126 %)

[a]The values in parenthesis represent the percentage of V_{max}/K_m compared with the corresponding value for wild-type FMO3.

[b]The values in parenthesis represent the percentage of V_{max}/K_m compared with the corresponding value for wild-type FMO1.

Kruskal-Wallis statistical analysis was run in order to compare values for FMO3 variants.** $p<0.01$ vs. values for wild-type FMO3 enzyme.

Mann Whitney test was run in order to compare values for FMO1 variant with wild-type enzyme †$p<0.05$ vs. value for wild-type FMO1 enzyme.

DMD Fast Forward. Published on September 19, 2006 as DOI: 10.1124/dmd.106.010827
This article has not been copyedited and formatted. The final version may differ from this version.

TABLE 3

S-Oxygenation of MMI by human FMO3 in the presence of Chlorpromazine.

The *S*-oxygenation of MMI in the presence of chlorpromazine was determined by monitoring the consumption of NADPH as described in *Materials and Methods*.

Data are mean ± standard deviation.

Enzyme	**Control Rate** (*nmol/min/mg of FMO3 protein*)	***Rate + Chlorpromazine***[a] (*nmol/min/mg of FMO3 protein*)	**Percent Increase**
FMO3 MBP	5.8 ± 0.2	7.2 ± 0.4	24.1***
Ala^{360}-FMO3 MBP	6.2 ± 0.1	6.7 ± 1.0	8.1
His^{360}-FMO3 MBP	7.2 ± 0.2	7.3 ± 0.6	1.2
Gln^{360}-FMO3 MBP	6.1 ± 0.2	6.9 ± 0.4	13.2
Pro^{360}-FMO3 MBP	4.6 ± 0.3	4.9 ± 0.5	5.8

[a] MMI was present at 2 mM and chlorpromazine was present at 1 mM. [b]The rate of MMI *S*-oxygenation in the presence of chlorpromazine was compared to the control rate obtained in the absence of chlorpromazine. Two way ANOVA was run in order to determine the effect of FMO3 isoform and modulator on enzyme activity and the interaction of these factors. Bonferroni post-test was done. ***$p<0.001$ vs. value for FMO3 enzyme variant in the absence of chlorpromazine.

DMD Fast Forward. Published on September 19, 2006 as DOI: 10.1124/dmd.106.010827
This article has not been copyedited and formatted. The final version may differ from this version.

TABLE 4

N-Oxygenation of tertiary amines by human FMO3.

(**A**) The *N*-oxygenation of 5-DPT in the presence of chlorpromazine was determined by monitoring formation of product by HPLC. (**B**) The N-oxygenation of Chlorpromazine in the presence of 5-DPT was determined by HPLC as described in *Materials and Methods.*

Condition	FMO3 MBP	Ala^{360}-FMO3 MBP	His^{360}-FMO3 MBP	Gln^{360}-FMO3 MBP	Pro^{360}FMO3 MBP
A. 5-DPT	62.2 ± 5.2	23.5 ± 0.9	4.4 ± 0.2	16.9 ± 0.5	61.1 ± 2.4
5-DPT + Chlorpromazine	62.9 ± 0.8	27.1 ± 1.9	5.3 ± 0.1	19.7 ± 0.1	62.9 ± 2.1
Percent increase	1.0	15.3	20.05	16.6	2.9
B. Chlorpromazine	43.6 ± 0.2	18.2 ± 0.2	5.2 ± 0.2	13.9 ± 0.2	41.6 ± 0.2
Chlorpromazine + 5-DPT	4.9 ± 0.2	2.1 ± 0.2	2.5 ± 0.2	1.5 ± 0.2	4.4 ± 0.2
Percent decrease	88.8***	88.5***	51.9***	89.2***	89.4***

[a]Rate of product formation expressed as nmol/min/mg of FMO3. [b]The rate of 5-DPT N-oxide formed in the presence of chlorpromazine was compared to the control rate obtained in the absence of chlorpromazine. [c]The rate of formation of chlorpromazine N-oxide in the presence of 5-DPT was compared to the control rate obtained in the absence of 5-DPT. Two way ANOVA was run in order to determine the effect of isoform and modulator on enzyme activity and the interaction of these factors. Bonferroni post-test was done. ***$p<0.001$ vs. value for FMO3 enzyme variants in the absence of 5-DPT.

DMD Fast Forward. Published on September 19, 2006 as DOI: 10.1124/dmd.106.010827
This article has not been copyedited and formatted. The final version may differ from this version.

Figure 1.

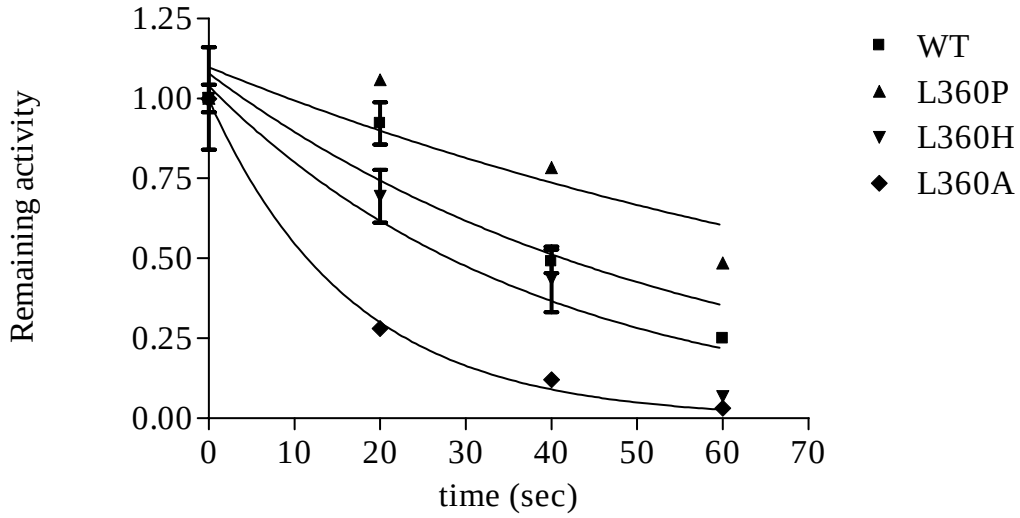

DMD Fast Forward. Published on September 19, 2006 as DOI: 10.1124/dmd.106.010827
This article has not been copyedited and formatted. The final version may differ from this version.

Figure 2

DMD Fast Forward. Published on September 19, 2006 as DOI: 10.1124/dmd.106.010827
This article has not been copyedited and formatted. The final version may differ from this version.

Figure 3